

An optimal 9-point, finite-difference, frequency-space, 2-D scalar wave extrapolator

Churl-Hyun Jo*, Changsoo Shin*, and Jung Hee Suh[‡]

ABSTRACT

In this study, a new finite-difference technique is designed to reduce the number of grid points needed in frequency-space domain modeling. The new algorithm uses optimal nine-point operators for the approximation of the Laplacian and the mass acceleration terms. The coefficients can be found by using the steepest descent method so that the best normalized phase curves can be obtained.

This method reduces the number of grid points per wavelength to 4 or less, with consequent reductions of computer memory and CPU time that are factors of tens less than those involved in the conventional second-order approximation formula when a band type solver is used on a scalar machine.

MOTIVATION

Numerical modeling of the wave equation in the frequency-space domain was pioneered by Lysmer and Drake (1972) and has been developed by Marfurt (1984) Shin (1988), Marfurt and Shin (1989) Pratt and Worthington (1990) and Pratt (1990a, b). Finite-element modeling in the frequency domain has been extensively upgraded by Marfurt and his colleagues (Marfurt 1988, personal communication).

Wave equation modeling in the time domain is popular because of its easy implementation and accuracy, compared to frequency domain modeling. The advantage of frequency-domain modeling over time-domain modeling is that multi-experiment seismic data can be simulated economically by direct multiplication once the triangular factors of the impedance matrix are calculated. Modeling the effects of attenuation is more flexible in the frequency domain than in the time domain (Pratt, 1990b), because in the frequency domain one can directly input the attenuation coefficient as a function of frequency. Furthermore, for certain geome-

tries, only a few frequency components are required to perform wave-equation inversion and tomography (Pratt and Worthington, 1990).

Because of numerical dispersion and anisotropy, the numerical solution of the wave equation can lead to inaccurate results. Such errors can be overcome by generating a sufficiently fine grid compared to the wavelength. In time-domain modeling, higher-order differencing operators are used to reduce the required spatial sampling (Dablain, 1986). For the conventional second-order central finite-difference operator used by Pratt and Worthington (1990), more grid points per wavelength are needed in frequency-domain solutions to obtain an accuracy that is comparable to that achieved with time-domain solutions. Moreover, the fact that frequency-domain modeling can be done only implicitly makes the problem harder because of the huge resultant matrix.

In this paper, several techniques are employed to increase the accuracy of frequency-domain modeling; these being (1) exploiting the extended Laplacian difference operator to reduce numerical anisotropy, (2) combining the mass acceleration term into the point collocation and weighted average term (Marfurt, 1984) and (3) finding averaging coefficients using the steepest descent method so that the best normalized phase curves can be obtained.

ACCURACY OF NUMERICAL MODELING

The scalar wave equation for a homogeneous isotropic medium in the frequency domain is

$$\nabla^2 P + \frac{\omega^2}{v^2} P = 0, \quad (1)$$

where P = the pressure wavefield, ω = the angular frequency, and v = velocity.

When the conventional second-order, central finite-difference, five-point approximation is applied to the Laplacian term in two dimensions, equation (1) becomes

Manuscript received by the Editor May 5, 1995; revised manuscript received August 9, 1995.

*Korea Institute of Geology, Mining, and Materials, P.O. Box 111, Taedok Science Town, Korea 305-350.

‡Department of Petroleum and Mineral Engineering, Seoul National University, Seoul, Korea, 151-742.

© 1996 Society of Exploration Geophysicists. All rights reserved.

$$\frac{P_{m+1,n} - 2P_{m,n} + P_{m-1,n}}{\Delta x^2} + \frac{P_{m,n+1} - 2P_{m,n} + P_{m,n-1}}{\Delta z^2} + \frac{\omega^2}{v^2} P_{m,n} = 0, \quad (2)$$

where $P_{w,n}$ represents the pressure of the wavefield at the location $[x_m, z_n] = [x_0 + (m-1)\Delta x, z_0 + (n-1)\Delta z]$. Figure 1 shows this grid.

Since exploration seismology requires relating events in time to horizons in depth, one concern is to minimize numerical velocity or dispersion errors (Alford et al., 1974; Marfurt, 1984). Dispersion analysis (Appendix A) allows an estimation of the accuracy of the solution in the frequency domain. Figures 2 and 3 compare dispersion curves corresponding to frequency-domain and time-domain algorithms. Since dispersion in the frequency domain is greater than that in the time domain, more grid points per wavelength should be used in the frequency domain to obtain an accuracy that is comparable to that of explicit time-domain extrapolation.

A NEW FINITE-DIFFERENCE SCHEME

To get more accurate results with the same, or a smaller number of, grid points per wavelength, a different implementation is suggested.

The first step is to generalize the Laplacian term

$$\nabla^2 P = a \nabla_{(0)}^2 P + (1-a) \nabla_{(45)}^2 P, \quad (3)$$

where

$$\nabla_{(0)}^2 P = \frac{\partial^2 P}{\partial x^2} + \frac{\partial^2 P}{\partial z^2},$$

$$\nabla_{(45)}^2 P = \frac{\partial^2 P}{\partial x'^2} + \frac{\partial^2 P}{\partial z'^2},$$

and the (x', z') coordinate system is rotated 45° relative to the (x, z) system. Finite-difference approximations to these operators can be expressed as

$$\nabla_{(0)}^2 P|_{x=x_m, z=z_n} = \frac{P_{m+1,n} + P_{m-1,n} - 4P_{m,n} + P_{m,n+1} + P_{m,n-1}}{\Delta^2}$$

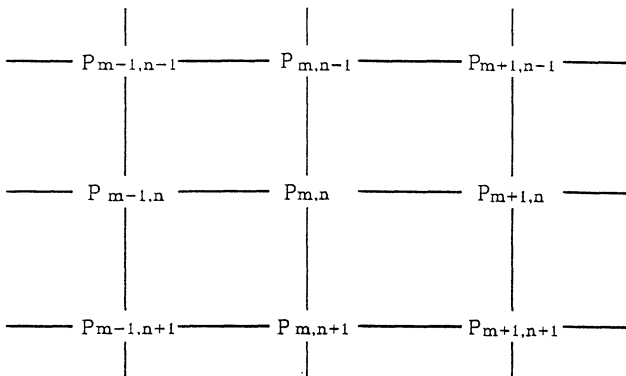


FIG. 1. The pressure fields P at the collocation point (m, n) and its eight nearest neighbors in a 2-D medium.

and

$$\nabla_{(45)}^2 P|_{x=x_m, z=z_n} = \frac{P_{m+1,n+1} + P_{m-1,n+1} - 4P_{m,n} + P_{m+1,n-1} + P_{m-1,n-1}}{(\sqrt{2}\Delta)^2},$$

where $A = AX = AZ$.

This generalization makes a nine-point Laplacian operator (Figure 4). With this formulation, the dispersion curves are calculated with $a = 0.5$. The result (Figure 5) shows relatively small numerical anisotropy with respect to propagation angle even though the method is, in general, less accurate than the conventional technique shown in Figure 2. The dispersion is maximum at a propagation angle of 45° and minimum at 0°. This difference can be explained by the fact that the grid interval of the 45° rotated coordinate system is larger than that of the 0° system.

The second step is to modify the technique used by Marfurt (1984) in which he considered the mass acceleration term to be a linear combination of the lumped mass matrix and the consistent mass matrix. Using this technique, the finite-difference approximation of the collocation point P of the mass

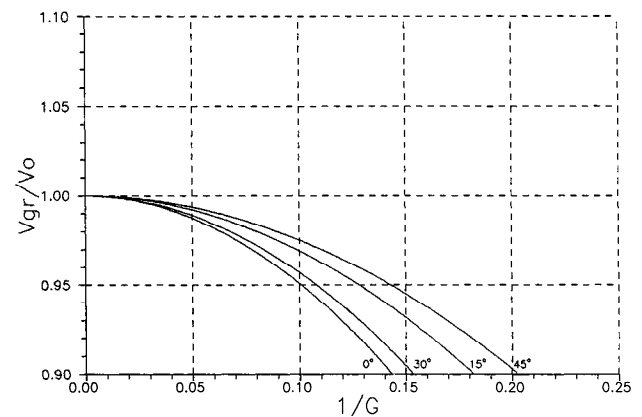
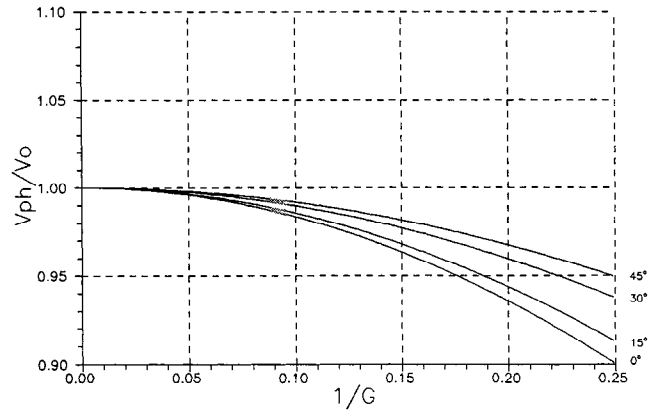


FIG. 2. Dispersion curves for finite-difference solution of the scalar 2-D wave equation in the frequency-space domain. Numerical phase velocity V_{ph} and numerical group velocity V_{gr} are normalized with respect to the true velocity V_0 and plotted versus wavenumber $k^* = k\Delta x/2\pi = \Delta x/\lambda = 1/G$, where G is the number of grid points per wavelength.

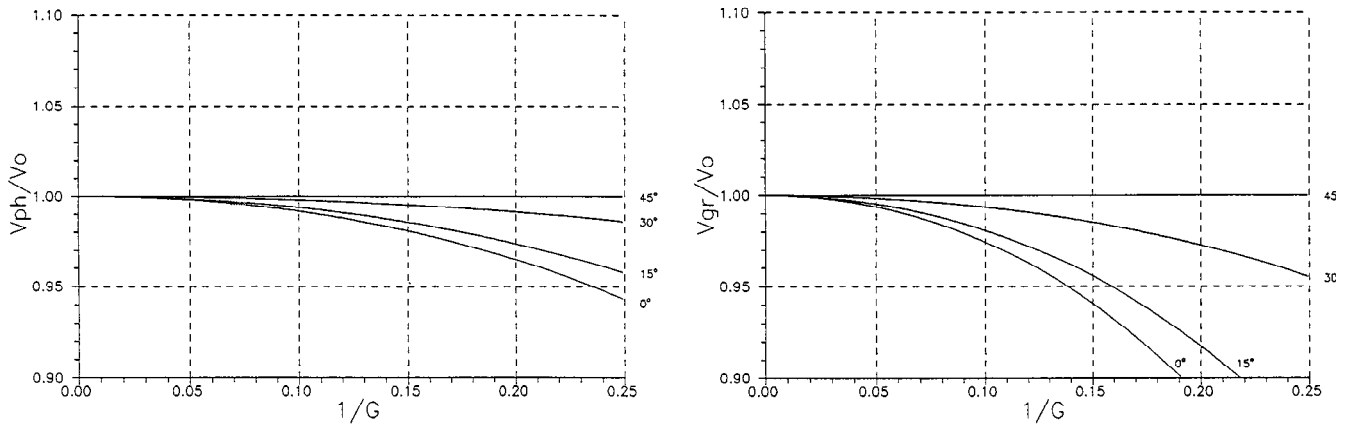


FIG. 3. Normalized phase V_{ph} and group V_{gr} velocity curves for different propagation angles with respect to the grid, for the explicit second-order central finite-difference scheme in time-space domain when the stability limit, $p = c\Delta t/\Delta x = 1/\sqrt{2}$, where c is the velocity.

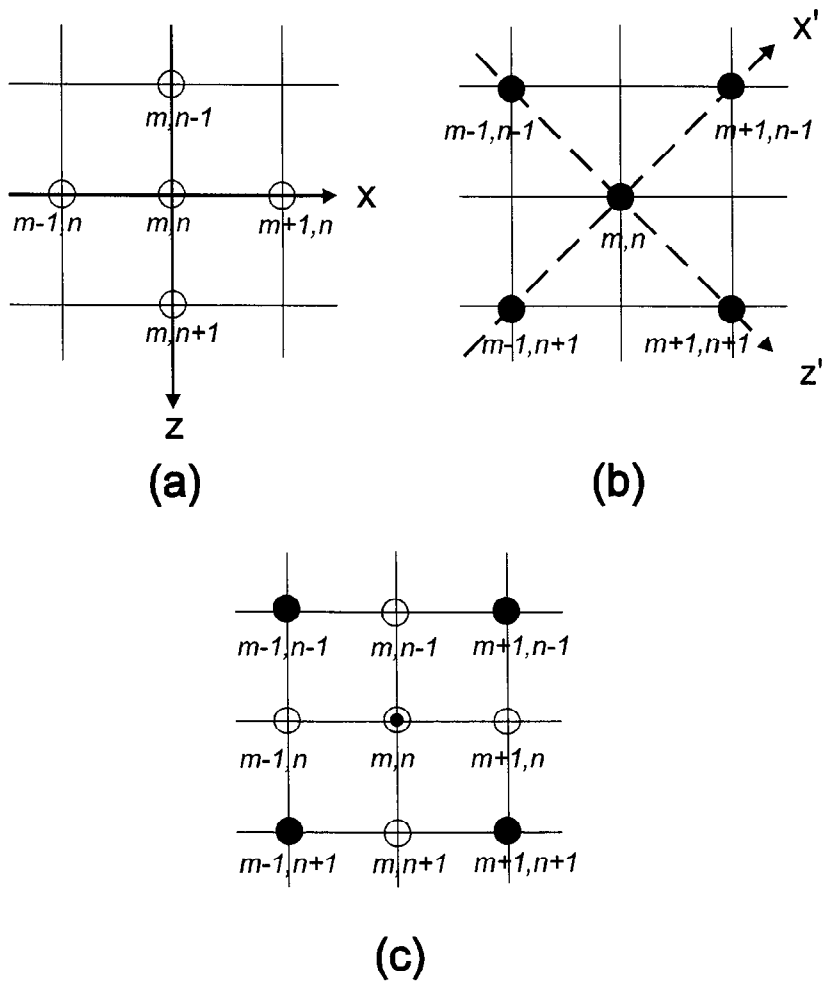


FIG. 4. Finite-difference stars for the Laplacian operator. (a) Conventional second-order central difference (five-point) star, (b) 45° rotated star, (c) nine-point star combining (a) and (b).

acceleration term $\omega^2/v^2 P$ in equation (1) can be represented as a linear combination of the points corresponding to the Laplacian operators, so that

$$P|_{m,n} = bP_{m,n} + \frac{(1-b)}{4} \times (P_{m+1,n} + P_{m-1,n} + P_{m,n+1} + P_{m,n-1}). \quad (4)$$

In practice the averaging coefficient b can be found by optimization (See Appendix B) in a manner similar to that used in Holberg (1987) to obtain optimal differencing operators in time domain modeling. Dispersion curves based on the optimized constant, $b = 0.737$, are shown in Figure 6. In this figure, dispersion curves are clustered on either side of the lines $V_{ph}/v = 1$ and $V_{gr}/v = 1$, which means that the numerical velocity does not diverge significantly from the true medium velocity.

Finally, by combining these two techniques we can expect more accurate results. The quantity P in the mass acceleration term $\omega^2/v^2 P$, in conjunction with the nine-point Laplacian operator, is

$$P|_{m,n} = cP_{m,n} + d(P_{m+1,n} + P_{m-1,n} + P_{m,n+1} + P_{m,n-1}) + e(P_{m+1,n+1} + P_{m-1,n+1} + P_{m+1,n-1} + P_{m-1,n-1}), \quad (5)$$

where $c + 4d + 4e = 1$.

Substitution of equations (5) and (3) into equation (1) gives the following difference equation

$$a \frac{(P_{m+1,n} + P_{m-1,n} - 4P_{m,n} + P_{m,n+1} + P_{m,n-1})}{\Delta^2} + (1-a) \times \frac{(P_{m+1,n+1} + P_{m-1,n+1} - 4P_{m,n} + P_{m+1,n-1} + P_{m-1,n-1})}{\Delta^2} + \frac{\omega^2}{v^2} \left[cP_{m,n} + d(P_{m+1,n} + P_{m-1,n} + P_{m,n+1} + P_{m,n-1}) + \frac{(1-c-4d)}{4} \times (P_{m+1,n+1} + P_{m-1,n+1} + P_{m+1,n-1} + P_{m-1,n-1}) \right] = 0. \quad (6)$$

The coefficients are optimized by minimizing the numerical dispersion error of the phase velocity (See Appendix B).

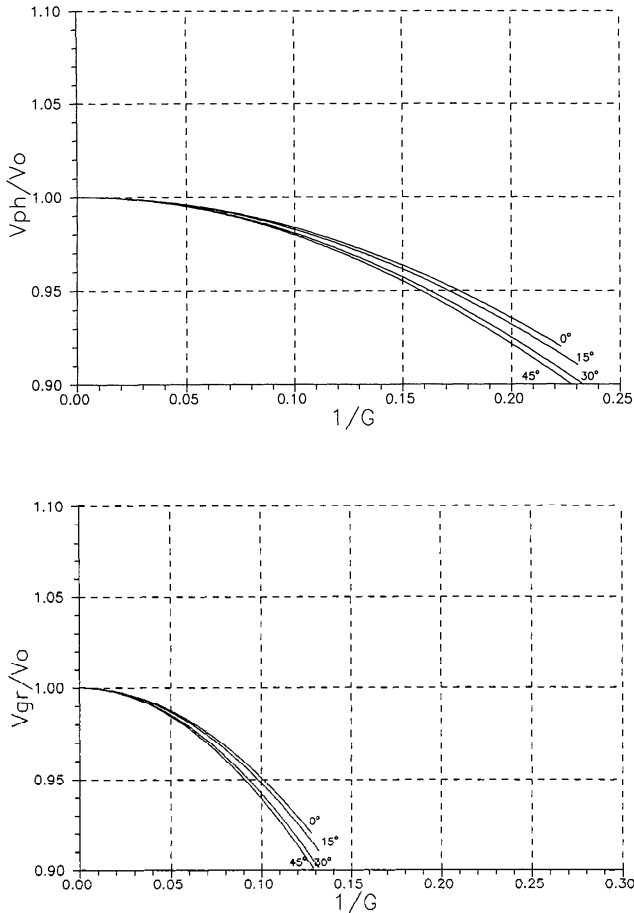


FIG. 5. Normalized phase V_{ph} and group V_{gr} velocity curves for finite-difference solutions in the frequency domain using the nine-point finite-difference formulation to approximate the Laplacian operator when $a = 0.5$ in equation (3).

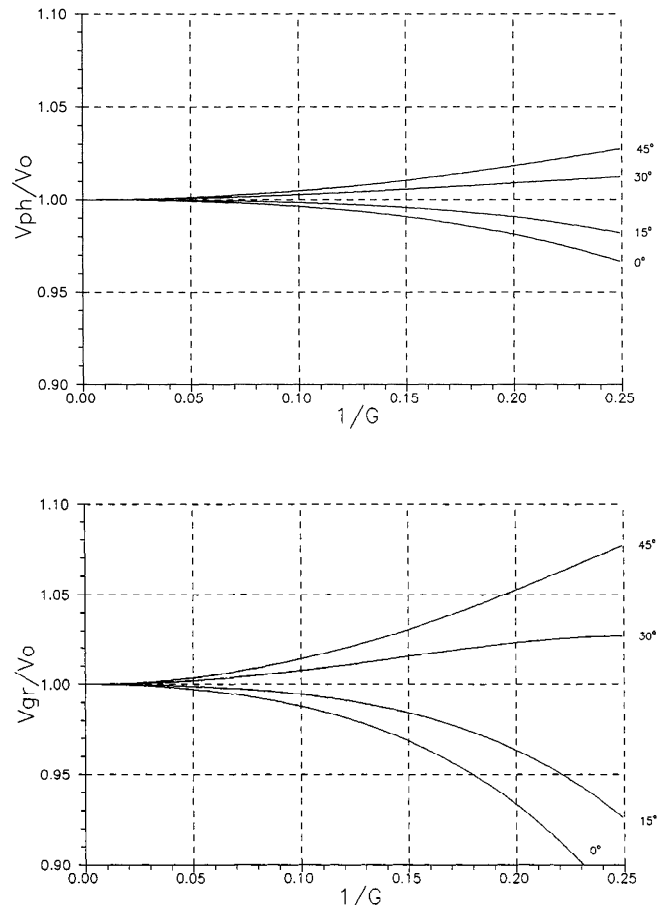


FIG. 6. Normalized phase V_{ph} and group V_{gr} velocity curves for frequency-domain, finite-difference solutions using an average term with $b = 0.7370$ in equation (4).

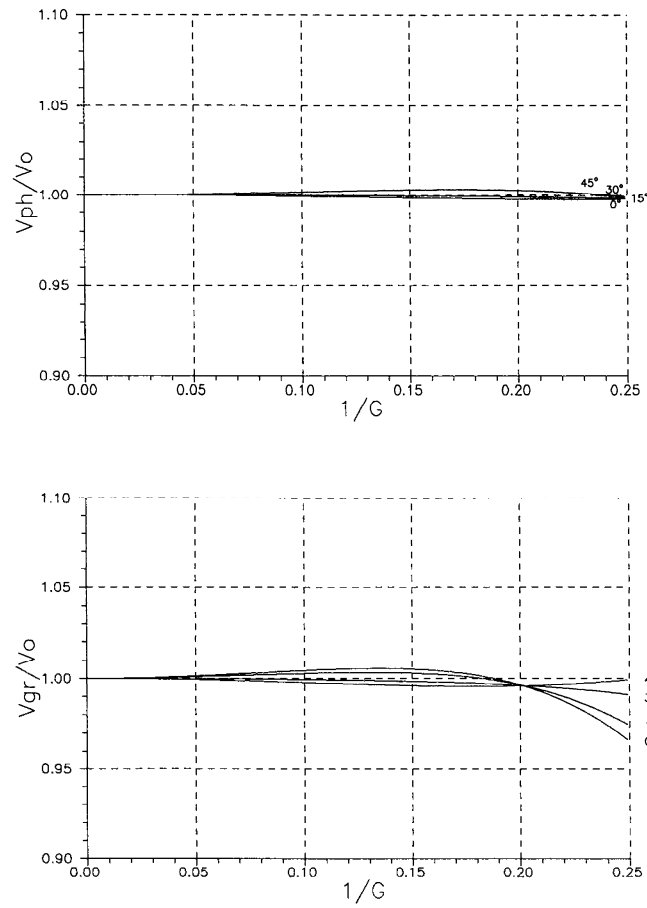


FIG. 7. Normalized phase V_{ph} and group V_{gr} velocity curves for frequency-domain, finite-difference solutions using the nine-point finite-difference formulation with $a = 0.5461$, $c = 0.6248$, and $d = 0.9381 \times 10^{-1}$ in equation (6).

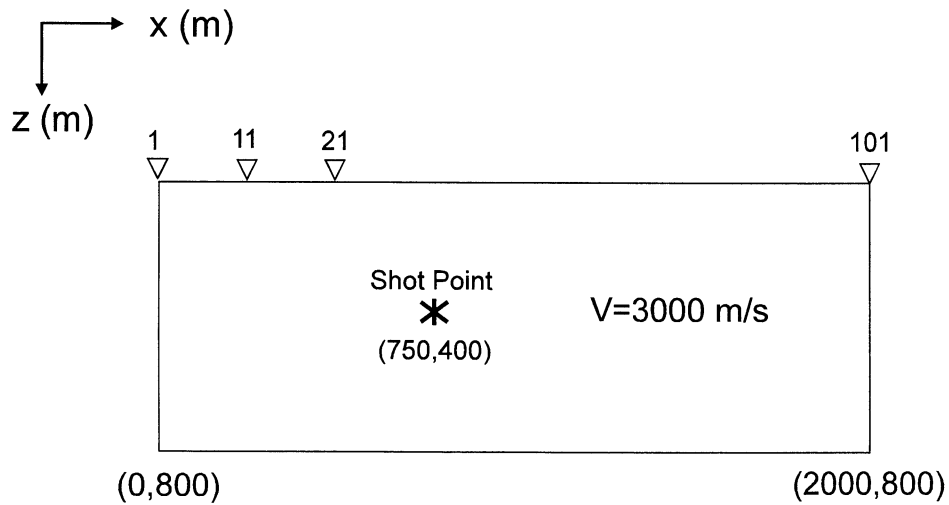


FIG. 8. A homogeneous half-space model to test the frequency-domain modeling. The velocity of the medium is 3000 m/s. The symbol $*$ denotes the shot point; every tenth receiver is shown with the symbol ∇ .

Numerical integration is done to calculate the residual error [equation (B-1)], using an interval of integration from 0° to 45° for angle θ , and 1/512 to 1/4 for wavenumber k^* . The optimized coefficients are $a = 0.5461$, $c = 0.6248$, and $d = 0.9381 \times 10^{-1}$. Dispersion curves based on these optimized coefficients are shown in Figure 7. When G_{min} , the number of grid points per shortest wavelength, is 4, the phase velocity error will be bounded within $\pm 0.5\%$, and when G_{min} is 3.2, the phase velocity error is bounded within $\pm 1\%$. For group velocity, this value will produce about 3% error. For a comparable degree of accuracy, the conventional five-point frequency-domain algorithm would have $G_{min} = 13$, while the explicit time-domain, finite-difference method would have $G_{min} = 10$.

We use a single active column matrix solver (Zienkiewicz, 1978) to factorize and solve the impedance matrix. Faster solutions would result if more efficient matrix solution methods, such as nested dissection (George and Liu, 1981) are used.

Time-domain seismograms are generated by Fourier synthesis; complex frequencies can be used to suppress the wrap-around effect of the Fast Fourier transform (FFT).

EXAMPLES

To examine the fidelity of solutions generated with the optimal nine-point, finite-difference formulation developed in this study, the conventional frequency-domain solution of Pratt and Worthington (1990) and the time-domain solution of Alford et al. (1974) are compared for the same homogeneous isotropic half-space model shown in Figure 8. The optimal averaging coefficients used are the same as those used in Figure 7; $G_{min} = 4$ in the frequency-domain calculations, $G_{min} = 9$ in the time domain, and the high-cut frequency of the source wavelet is 60 Hz. For the time-domain solution, second-order central finite differences are used to approximate the spatial derivatives. Time integration is performed explicitly and run at the stability limit, $p = c\Delta t/\Delta x = 1/\sqrt{2}$. The seismogram generated by the conventional five-point frequency-domain scheme (Figure 9a) shows evidence of dispersion because of insufficient nodal points, while the seismograms calculated by the optimal nine-point operator (Figure 9b), as well as those by explicit time-domain modeling (Figure 9c), show no apparent dispersion. Another example for a syncline model (Figure 10) illustrates the reflection characteristics of the optimal nine-point, finite-difference formulation. Results of time-domain modeling are presented for comparison. The results (Figure 11) look similar to each other, except for unstable signals at late times for near-shot receivers in the frequency-domain modeling (Figure 11a), which are caused by time aliasing of energy before time zero.

CONCLUSION

Numerical modeling in the frequency domain has not been widely used since the large matrix equations require large computer memories. These matrices can be reduced in size by using a more accurate scheme.

Our new scheme uses an optimal nine-point, finite-difference approximation of the Laplacian and mass acceleration terms. We admit that the frequency-domain modeling technique cannot compete with other modeling techniques, such as the Fourier method (Kosloff and Baysal, 1982) in modeling conventional synthetic sections. However, for certain problems (e.g., modeling structures with frequency-dependent physical properties and wave-equation tomography where only a small number of frequency components are used), this frequency-domain method will make the problem less expensive. Furthermore, the optimal finite-difference formulation, with a more efficient sparse matrix solver such as nested dissection, can further reduce the computational cost of such modeling.

ACKNOWLEDGMENTS

The research was inspired by Dr. K. R. Kelly of Amoco. We wish to thank Prof. B. K. Hyun and C. E. Baag of Seoul National University and Dr. S. H. Cheong of KIGAM for helpful discussions during the study. Dr. K. J. Marfurt of Amoco was kind enough to review the manuscript and to offer many suggestions that greatly improved the study. We are also grateful to Dr. R. G. Pratt of Imperial College and Prof. E. A. Robinson for their constructive comments on the manuscript.

REFERENCES

- Alford, R. M., Kelly, K. R., and Boore, D. M., 1974, Accuracy of finite-difference modeling of the acoustic wave equation: *Geophysics*, 39, 834-842.
- Cont, S. D., and de Boor, C., 1980, *Elementary numerical analysis*, 3rd ed.: McGraw-Hill Book Co.
- Dablain, M. A., 1986, The application of high-order differencing to the scalar equation: *Geophysics*, 51, 54 - 66.
- George, A., and Liu, J. W., 1981, *Computer solution of large sparse positive definite systems*: Prentice-Hall, Inc.
- Holberg, O., 1987, Computational aspect of the choice of operator and sampling interval for numerical differentiation in large-scale simulation of wave phenomena: *Geophys. Prosp.*, 35, 629-655.
- Kosloff, D. D., and Baysal, E., 1982, Forward modeling by a Fourier method: *Geophysics*, 47, 1402-1412.
- Lysmer and Drake, 1972, A finite-element method for seismology, in Bolt, B. A., Eds., *Methods in computational physics*, Volume 11: *Seismology: Surface waves and earth oscillations*: Academic Press Inc., 181-216.
- Marfurt, K. J., 1984, Accuracy of finite-difference and finite-element modeling of the scalar and elastic wave equations: *Geophysics*, 49, 533-549.
- Marfurt, K. J., and Shin, C. S., 1989, The future of iterative modeling in geophysical exploration, in Eisner, E., Ed., *Handbook of geophysical exploration: I Seismic Exploration*, Volume 21: *Supercomputers in seismic exploration*: Pergamon Press, 203-228.
- Pratt, R. G., 1990a, Inverse theory applied to multi-source cross-hole tomography, Part II: Elastic wave-equation method: *Geophys. Prosp.*, 38, 287-310.
- 1990b, Frequency-domain elastic wave modeling by finite differences: A tool for crosshole seismic imaging: *Geophysics*, 55, 626-632.
- Pratt, R. G., and Worthington, M. H., 1990, Inverse theory applied to multi-source cross-hole tomography, Part I: Acoustic wave-equation method: *Geophys. Prosp.*, 38, 287-310.
- Shin, C. S., 1988, *Nonlinear elastic wave inversion by blocky parameterization*: Ph.D. thesis, Univ. of Tulsa.
- Zienkiewicz, O. C., 1978, *The finite-element methods*, 3rd ed.: McGraw-Hill Book Co.

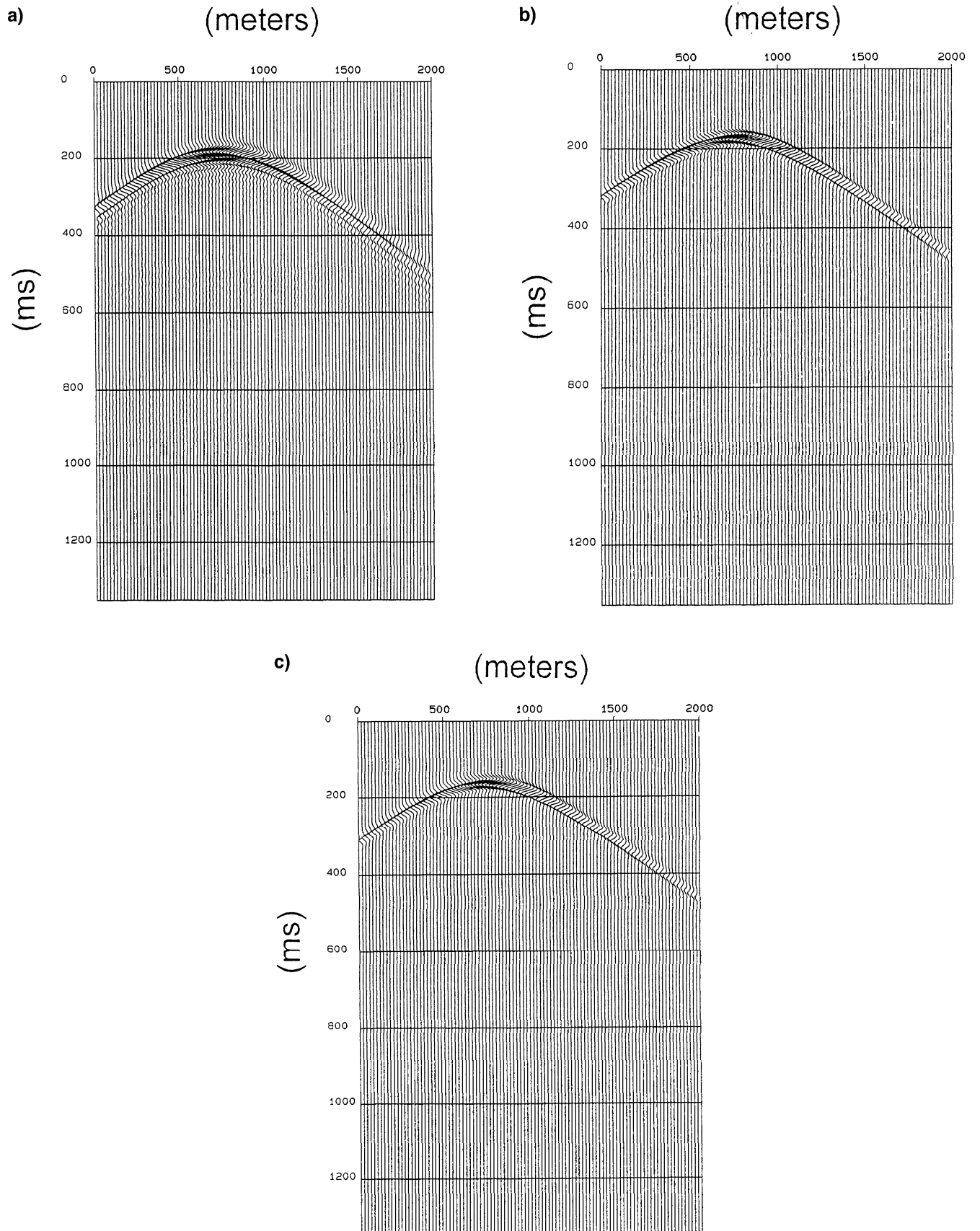


FIG. 9. Synthetic seismograms generated by the finite-difference solutions of the 2-D scalar wave equation for the homogeneous half-space model shown in Figure 8 by (a) the conventional frequency-domain method, (b) the frequency-aomam formula using the optimal nine-point finite differences, and (c) the explicit time-domain scheme (second-order central difference).

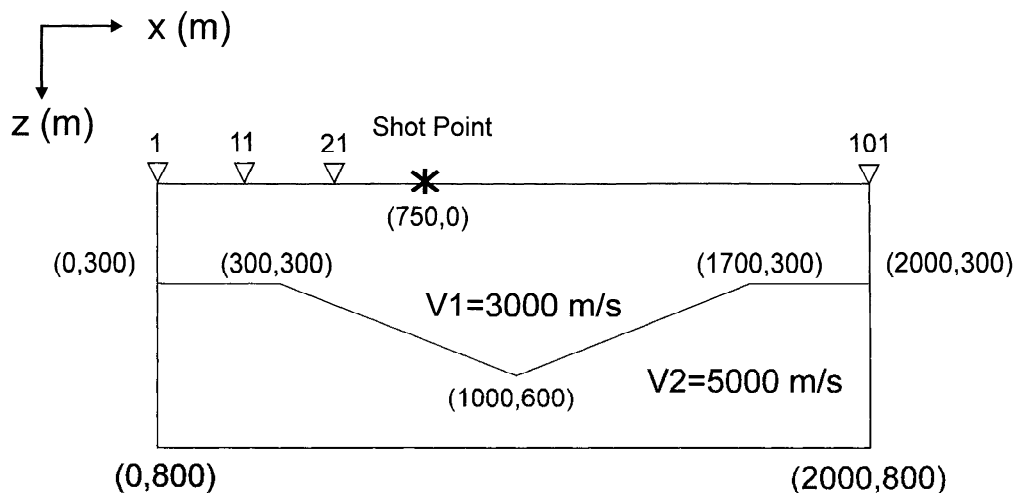


FIG. 10. Syncline model showing receiver and source geometry. $V_1 = 3000$ m/s, $V_2 = 5000$ m/s.

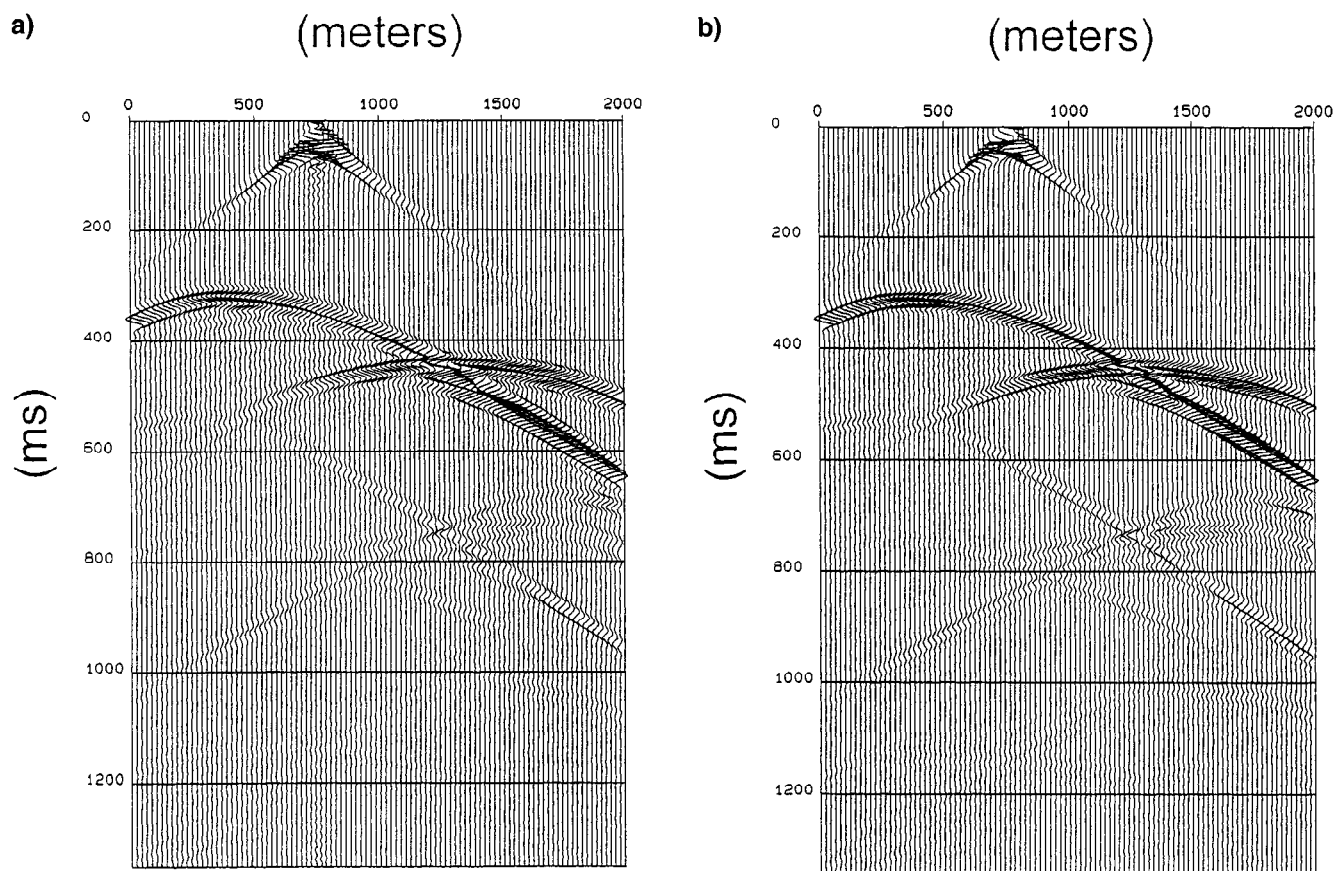


FIG. 11. Synthetic seismograms generated from the finite-difference solutions for the syncline model shown in Figure 10 by (a) the frequency-domain formula using the optimal nine-point finite differences, and (b) the explicit time-domain scheme. The shot point is located at 750 m.

APPENDIX A

DISPERSION ANALYSIS

Substituting a plane harmonic wave solution of the form

$$P(x, z, \omega) = P_0 e^{-i(k_x x + k_z z)}$$

into equation (6) gives the dispersion equation

$$\frac{\omega^2}{v^2} = \frac{a[4 - 2 \cos(k\Delta \cos \theta) - 2 \cos(k\Delta \sin \theta)] + (1-a)[2 - 2 \cos(k\Delta \cos \theta) \cos(k\Delta \sin \theta)]}{\Delta^2 \{c + 2d[\cos(k\Delta \cos \theta) + \cos(k\Delta \sin \theta)] + 4e \cos(k\Delta \cos \theta) \cos(k\Delta \sin \theta)\}}, \quad (\text{A-1})$$

where $\Delta (= \Delta x = \Delta z)$ is the grid interval, $c + 4d + 4e = 1$, and θ is the propagation angle from the z-axis. From the definition of phase and group velocities, $V_{ph} = \omega/k$ and $V_{gr} = \partial\omega/\partial k$, the normalized numerical phase and group velocities can be written as

$$\frac{V_{ph}}{v} = \frac{\left\{ a \left[\sin^2 \left(\frac{\pi \cos \theta}{G} \right) + \sin^2 \left(\frac{\pi \sin \theta}{G} \right) \right] + \frac{(1-a)}{2} \left[1 - \cos \left(\frac{2\pi \cos \theta}{G} \right) \cos \left(\frac{2\pi \sin \theta}{G} \right) \right] \right\}^{1/2}}{\frac{\pi}{G} \left\{ c + 2d \left[\cos \left(\frac{2\pi \cos \theta}{G} \right) + \cos \left(\frac{2\pi \sin \theta}{G} \right) \right] + 4e \cos \left(\frac{2\pi \cos \theta}{G} \right) \cos \left(\frac{2\pi \sin \theta}{G} \right) \right\}^{1/2}} \quad (\text{A-2a})$$

and

$$\frac{V_{gr}}{v} = \frac{v (B'A - BA')}{V_{ph} \frac{2\pi}{G} A^2}, \quad (\text{A-2b})$$

$$A' = -d \left[\cos \theta \sin \left(\frac{2\pi \cos \theta}{G} \right) + \sin \theta \sin \left(\frac{2\pi \sin \theta}{G} \right) \right]$$

$$- \frac{(1-c-4d)}{2} \left[\cos \theta \sin \left(\frac{2\pi \cos \theta}{G} \right) \cos \left(\frac{2\pi \sin \theta}{G} \right) \right.$$

$$\left. + \sin \theta \cos \left(\frac{2\pi \cos \theta}{G} \right) \sin \left(\frac{2\pi \sin \theta}{G} \right) \right]$$

where

v is the medium velocity,

$G = \frac{\lambda}{\Delta}$ = the number of grid points per wavelength,

$$A = c + 2d \left[\cos \left(\frac{2\pi \cos \theta}{G} \right) + \cos \left(\frac{2\pi \sin \theta}{G} \right) \right]$$

$$+ (1-c-4d) \cos \left(\frac{2\pi \cos \theta}{G} \right) \cos \left(\frac{2\pi \sin \theta}{G} \right),$$

$$B = a \left[4 - 2 \cos \left(\frac{2\pi \cos \theta}{G} \right) - 2 \cos \left(\frac{2\pi \sin \theta}{G} \right) \right]$$

$$+ \frac{(1-a)}{2} \left[4 - 4 \cos \left(\frac{2\pi \cos \theta}{G} \right) \cos \left(\frac{2\pi \sin \theta}{G} \right) \right],$$

and

$$B' = a \left[\cos \theta \sin \left(\frac{2\pi \cos \theta}{G} \right) + \sin \theta \sin \left(\frac{2\pi \sin \theta}{G} \right) \right]$$

$$(1-a) \left[\cos \theta \sin \left(\frac{2\pi \cos \theta}{G} \right) \cos \left(\frac{2\pi \sin \theta}{G} \right) \right.$$

$$\left. + \sin \theta \cos \left(\frac{2\pi \cos \theta}{G} \right) \sin \left(\frac{2\pi \sin \theta}{G} \right) \right].$$

APPENDIX B

OPTIMIZATION

Since numerical dispersion in 2-D depends on propagation angle as well as on grid size, the averaging coefficients a , c , and d in equations (6) and (A-2a) should be determined such that the L_2 norm of the residual error is minimized. When the error of numerical phase velocity is defined as

$$\varepsilon(\theta, k^*; a, c, d) = \left[1 - \frac{V_{ph}(\theta, k^*; a, c, d)}{v} \right]^2,$$

the L_2 norm of the residual to be minimized can be expressed as

$$E(a, c, d) = \int \int \varepsilon(\theta, k^*; a, c, d) dk^* d\theta, \quad (\text{B-1})$$

where $k^* = k\Delta/2\pi = \Delta/\lambda = 1/G$.

To obtain the optimal values of a , c , and d , the method of steepest descent had been applied to the minimization of E . By a general iterative rule (Cont and De Boor, 1980), the parameters a , c , and d are updated until the minimum of the objective function

$$p^{k+1} = p^k - \beta \nabla E(\mathbf{x}) \quad (\text{B-2})$$

is reached, where k is the iteration number, p is one of a , c , or d , and

$$\nabla E(\mathbf{x}) = \left[\frac{\partial E}{\partial a} \frac{\partial E}{\partial c} \frac{\partial E}{\partial d} \right]^T$$

is the gradient vector of $E(x)$.

Using equation (B-2), the averaging coefficients can be determined, minimizing the error defined as equation (B-1).